

Fingerprint Singular Point Detection Algorithm by Poincaré Index

Jin Bo, Tang Hua Ping, Xu Ming Lan
The College of Electrical and Information Engineering
Zhejiang Textile And Fashion College
No.495 Fenghua Road, Ningbo City, Zhejiang Province
CHINA

Abstract: - Fingerprint indexing is an efficient technique that greatly improves the performance of Automated Fingerprint Identification Systems. We propose a continuous fingerprint indexing method based on location, direction estimation and correlation of fingerprint singular points. There have been many approaches introduced in the design of feature extraction. Based on orientation field, Firstly, we divide it into blocks to compute the Poincaré Index. Then, the blocks which may have singularities are detected in the block images. Experiment show the present algorithm is robust than the traditional method on poor quality images.

Key-words: - Fingerprint Core Delta Point Orientation Poincaré Index

1 Introduction

Every person is believed to have unique fingerprints [1]. This makes fingerprint matching one of the most reliable methods for identifying people [2]. Fingerprint matching is usually carried out at two different levels. At the coarse level, fingerprints can be classified into six main classes: arch, tented arch, right loop, left loop, whorl and twin loop, as shown in Fig.1. The fine-level matching is performed by extracting ridge endings and branching points, called minutiae [3], from a fingerprint image. The similarity between two fingerprints is determined by comparing the two sets of minutiae points. Although the coarse classification does not identify a fingerprint uniquely, it is helpful in determining when two fingerprints do not match. For example, a right loop image should be matched with only other right loop images in the database of fingerprints. When fingerprints from all the ten fingers are available, the coarse level classification of these ten prints drastically reduces the proportion of database images to be matched at the finer level. A human expert can perform coarse-level classification of fingerprints relatively easy. For an automatic system, the problem is much more difficult because the system must take into account the global directions of the ridges as well as their local connectivity to make its decision.

In recent years, fingerprints are most widely used for personal identification. Fingerprint images are direction oriented patterns formed by ridges and

valleys. The singular point area is defined as a region where the ridge curvature is higher than normal and where the direction of the ridge changes rapidly. In most fingerprint identification algorithms and fingerprint classification algorithms, extracting the number and the precise location of SPs is of great importance.

Fingerprint classification is a coarse level partitioning of a large fingerprint database, where the class of the input fingerprint is first determined and subsequently, a search is conducted within the set of fingerprints belonging to the same class as the input fingerprint. In regard to fingerprint classification, only a portion of a fingerprint, called pattern area is of interest [4]. The pattern area of a fingerprint consists of those ridges encircled by typelines which is defined as the two innermost ridges that form a divergence tending to encircle or encompass the central portion of a fingerprint [5]. The pattern areas of loop or whorl types of fingerprints contain two types of singular points (core and delta). So it is very important to detect singular points accurately and reliably [6]. Nowadays, a practical method based on the Poincaré Index was always used for fingerprint singularities detection and a fingerprint has a well-defined orientation. The traditional detection based on the point orientation field can gain the accurate position of singularities, but the singular points are misjudged or not judged for the low quality image of the fingerprint sometimes and the



Arch



Tented Arch



Left Loop



Right Loop



Whorl



Twin-Loop

Fig. 1. Six classes of fingerprints

Algorithm has a high computational complexity. However, the traditional detection based on the block orientation field can detect the existence of all the singular points, but can not locate the positions accurately. The classical formula to compute the Poincaré Index can present only the rotation angles, but not the rotation direction of the vector in the vector field exactly.

We propose a multi-scale detection algorithm for singular points in fingerprint images based on both the continuous orientation field and the modified Poincaré Index. Firstly, the blocks which may contain singularities are detected by computing the Poincaré Index. Then, the singularities are detected in the block images accurately and reliably. So the new algorithm can locate the singularities at pixel level with an accuracy of only one pixel.

The main steps of our structural approach to fingerprints classification are as follows:

- 1) Computation of the directional image of the fingerprints. This directional image is a 28×30 matrix. Each matrix element represents the ridge orientation within a given block of the input image. The directional image was computed using the algorithm proposed in Ref. [7].
- 2) Segmentation of the directional image into regions containing ridges with similar orientations. To this end, the segmentation algorithm described in Ref. [8] was used.

2 Image segment

The boundary region, surrounding the actual fingerprint in the image, inherently contains discontinuities in the ridge pattern since beyond that boundary is background with relatively constant (but often noisy) pixel intensity. To address the border discontinuities, the fingerprint is segmented from the background.

We use the blockwise coherence to segment the images. The block is considered as foreground if its coherence of its direction field satisfy some predefined threshold, otherwise, the background. Then two iterations of dilation and erosion are used to remove holes resulting from inhomogenous regions. All the process discussed below is carried out on such foreground regions.

3 The coherence of Orientation field

Let $I(i, j)$ denote the gray level of the pixel (i, j) in a $M \times N$ fingerprint image. Let $\theta'(x, y)$ represent the orientation of the anisotropy of the non-overlapping block centered at (x, y) , and $\theta(x, y)$ the local

dominant orientation (or flow direction). The local dominant orientation $\theta(x, y)$ equals $\theta'(x, y) + \pi/2$ since the flow orientation is perpendicular to the direction of anisotropy. For fingerprint images, in case the opposite directions cancel each other out, we define the range of the direction angles as $(0, \pi)$. Let $\chi(x, y)$ represent the coherence of the flow directions.

Since the gradients of a Gaussian filter can give a good estimate of the underlying oriented pattern, we adopt its orientation as the local direction. First, the image is convolved with a Gaussian filter whose impulse response is given by

$$g_1(x, y) = e^{-(x^2+y^2)/2\sigma^2} \tag{1}$$

The filtered image is expressed as

$$G(i, j) = g_1(i, j) \times I(i, j) \tag{2}$$

Next, the optimal 3 by 3 operators [9] are used to obtain the gradients in horizontal and vertical directions as $G_x(i, j)$ and $G_y(i, j)$. Thus, the amplitude of the gradient is

$$|G(i, j)| = \sqrt{G_x^2(i, j) + G_y^2(i, j)} \tag{3}$$

Let

$$\begin{cases} J_1(i, j) = 2G_x(i, j)G_y(i, j) \\ J_2(i, j) = G_x^2(i, j) - G_y^2(i, j) \\ J_3(i, j) = G_x^2(i, j) + G_y^2(i, j) \end{cases} \tag{4}$$

then, the anisotropy orientation estimate of the 8 by 8 block (x, y) is

$$\bar{\theta}(x, y) = \frac{1}{2} \tan^{-1} \left(\frac{\sum_{(i,j) \in \Phi_1} J_1(i, j)}{\sum_{(i,j) \in \Phi_1} J_2(i, j)} \right) \tag{5}$$

where Φ_1 is smoothing window centered on the block with the size of W_1 by W_1 [10,11]. For fingerprint images, the average width of the ridge or valley is five to eight pixels, so $W_1 = 16$ gives a good orientation estimate and saves computational time. Furthermore,

$$\theta(x, y) = \bar{\theta}(x, y) + \frac{\pi}{2} \tag{6}$$

However, there are two reasons for failure of the orientation measure [11]. The neighborhood may contain a constant gray value area or an isotropic gray value structure without a preferred orientation. To distinguish these two cases we need to compare the magnitude of the orientation vector with the mean square magnitude of the gradient. As to fingerprint images, the background shows constant gray value, if

we can distinguish between them, our segmentation will be ready. Therefore, we first set the threshold value G_{th} of the Gradient as

$$G_{th} = g_t * (|G_i|_{max} - |G_i|_{min}) + |G_i|_{min} \quad (7)$$

where $|G_i|_{max}$ and $|G_i|_{min}$ are supposed to be the global maximum and minimum gradient amplitude of the image respectively, and g_t is the threshold factor [12]. Smaller values of g_t will encourage weak edges to be identified, while larger values will favor noise suppression. For varied contrast fingerprint images, g_t is selected in the range of [0.05, 0.3]. In our work, $|G_i|_{max}$ and $|G_i|_{min}$ are adjusted in order to avoid the effect of asymmetry of the gradient distribution.

Therefore, the block coherence is defined as

$$\chi(x, y) = \begin{cases} -1, & \text{if } \frac{1}{w_1 * w_1} \sum_{(i,j) \in \phi_1} J_3(i, j) < G_{th} * G_{th} \\ \left(\frac{\left(\sum_{(i,j) \in \phi_1} J_1(i, j) \right)^2 + \left(\sum_{(i,j) \in \phi_1} J_2(i, j) \right)^2}{\sum_{(i,j) \in \phi_1} J_3(i, j)} \right)^{\frac{1}{2}} & \end{cases} \quad (8)$$

The block is regarded as a candidate for the background if the coherence is -1 . The coherence ranges from 0 to 1. For ideal local orientation it is one, for an isotropic gray value structure without a preferred orientation it is zero which is correspondent to the noisy regions in the foreground or the regions near core or delta.

We then label all the connected regions whose coherence values are not 1, choose the one with the largest area as the supposed foreground print area. For the supposed background regions, if they are surrounded by the foreground, they are labeled as noisy regions or low contrast regions. Whose coherences are assigned a value of zero. That is

$$\chi'(x, y) = \begin{cases} -1 & \text{background} \\ 0 & \text{noisy} \\ \chi(x, y) & \text{foreground} \end{cases} \quad (9)$$

The average coherence of the foreground indicates the clarity of ridges, therefore, it can be used to control the reject rate if needed.

In this process, not only are the fingerprint ridge orientation and coherence attained, but the image is

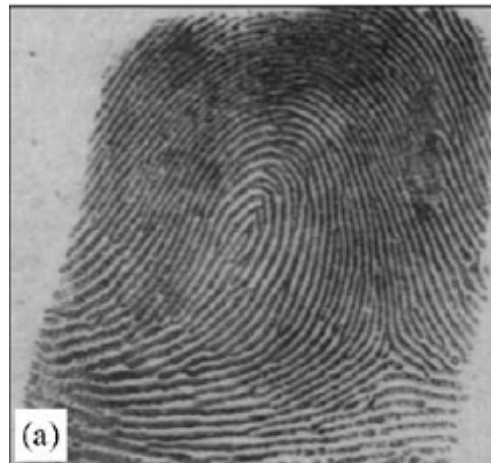
also segmented into noisy, background or foreground regions as a by-product. It is better than other methods as they treat all the blocks the same without separating the constant gray value area from the isotropic gray value structure without a preferred orientation.

4 The eight direction field

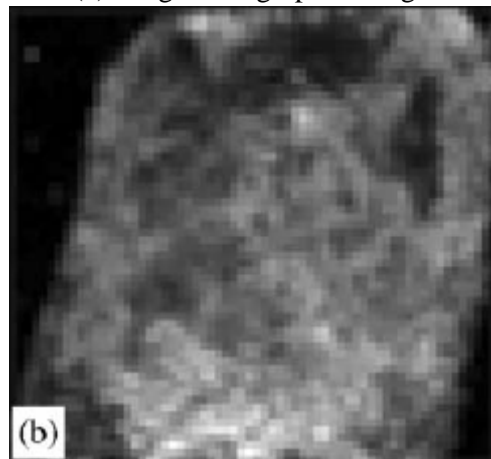
A fingerprint has a well-defined direction field [13]. To compute the direction field, we define the ridge direction of a pixel as 8 directions. (at positions marked by numbers 1, ..., 8).

To decide the ridge direction of each pixel in the image, we compute the average grey value in direction i ($i=1, \dots, 8$ means one of the 8 directions) in a 9×9 window with the pixel as the centre. We compute the average grey value of the pixels labelled "i" and obtained $G[i]$. The 8 mean grey values are divided into 4 groups with the two directions in each group perpendicular to each other. Group j ($j=1, 2, 3, 4$) contains direction j and $j+4$. The absolute value of the difference of the mean grey value is calculated in each group as:

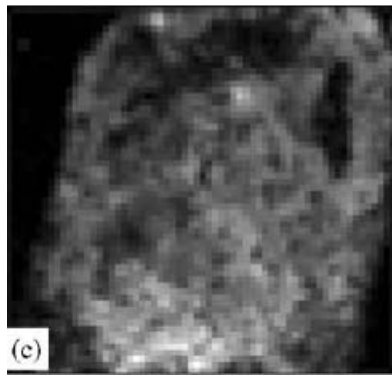
$$G_{diff}[j] = |G_{mean}[j] - G_{mean}[j+4]| \quad (j=1, 2, 3, 4) \quad (10)$$



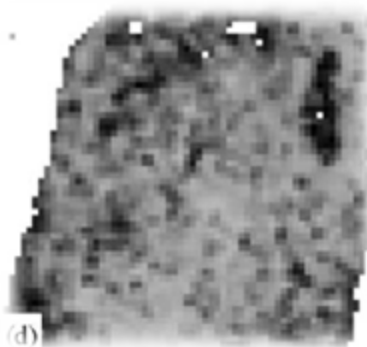
(a) Original fingerprint image



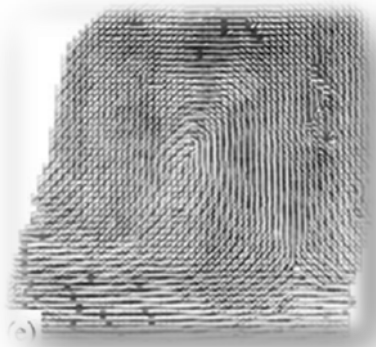
(b) mean-square of the gradient (gt = 0.15)



(c) orientation certainty



(d) coherence



(e) orientation overlaid on the segmented image

Fig. 2. Results of orientation field computation as well as image segmentation

7		6		5		4		3
8		7	6	5	4	3		2
		8				2		
1		1		*		1		1
		2				8		
2		3	4	5	6	7		8
3		4		5		6		7

Fig.3 eight direction

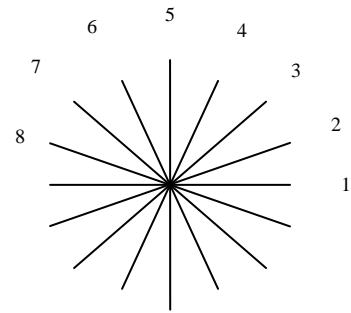


Fig.4 ridge directions of a pixel

Set the two directions in the group with the largest difference value as possible ridge direction. If

$$i_{max} = \arg \left\{ \text{Max}_{i \in \{0,1,2,3\}} (G_{diff}(i)) \right\} \quad (11)$$

then i_{max} and i_{max+4} are possible ridge directions. The ridge direction in the pixel is decided by

$$o(x, y) = \begin{cases} i_{max} & \text{if } |Grey - G[i_{max}]| \\ < |Grey - G[i_{max+4}]| \\ i_{max+4} & \text{otherwise} \end{cases} \quad (12)$$

Where $Grey$ is the grey value at this pixel.

To reduce noise, the point direction field is smoothed. A local window of size 17×17 is taken around each pixel, keeping it as the central of the window. We set the ridge direction of each pixel in the window as the direction of that pixel. That is, the mean direction of all the pixels in the window. To obtain the mean direction of a window, we calculate the number of pixels in the window where ridge direction is estimated as $i(i=1, \dots, 8)$ and set this number as $N[i]$. The mean direction of the block is:

$$O(x, y) = \arg \left\{ \text{Max}_{i=\{1, \dots, 8\}} (N[i]) \right\} \quad (13)$$

The smoothed point orientation field $O(x,y)$ is also called the continuous direction field [14].

We divided the continuous field into small blocks of size 9×9 and set the ridge direction of each pixels in the block as the mean direction of all the pixels in the block. To obtain the mean direction of a block, we calculate the number of pixels in the block where ridge direction is estimated as $i(i=1, \dots, 8)$ and set this number as Ni . The mean direction of the block is:

$$M(i, j) = \arg \left\{ \text{Max}_{i=\{1, \dots, 8\}} (Ni) \right\} \quad (14)$$

The block orientation field is a matrix and every pixel is estimated as $j(j=1, \dots, 8)$.

5 Direction estimation by least mean square

A number of methods have been developed to estimate the orientation field in a fingerprint [15]–[18]. The least mean square orientation estimation algorithm [19] has the following steps.

- 1) Divide I, the input image, into nonoverlapping blocks of size $w \times w$.
- 2) Compute the gradients $\partial x(i, j)$ and $\partial y(i, j)$ at each pixel (i, j) . Depending on the computational requirement, the gradient operator may vary from the simple Sobel operator to the more complex Marr–Hildreth operator [20].
- 3) Estimate the local orientation of each block centered at pixel (i, j) using the following equations [18]:

$$v_x(i, j) = \sum_{u=i-w/2}^{i+w/2} \sum_{v=j-w/2}^{j+w/2} 2\partial_x(u, v)\partial_y(u, v)$$

$$v_y(i, j) = \sum_{u=i-w/2}^{i+w/2} \sum_{v=j-w/2}^{j+w/2} (\partial_x^2(u, v) - \partial_y^2(u, v)) \quad (15)$$

$$o(i, j) = \frac{1}{2} \tan^{-1} \left(\frac{v_y(i, j)}{v_x(i, j)} \right)$$

where $o(i, j)$ is the least square estimate of the local ridge orientation at the block centered at pixel (i, j) . Mathematically, it represents the direction that is orthogonal to the dominant direction of the Fourier spectrum of the $w \times w$ window.

A summary of our algorithm is presented below.

- 1) Estimate the orientation field o as described above using a window size of $w \times w$.
- 2) Smooth the orientation field in a local neighborhood. Let the smoothed orientation field be represented as o' . In order to perform smoothing (low-pass filtering), the orientation image needs to be converted into a continuous vector field, which is defined as follows:

$$\Phi_x(i, j) = \cos 2o(i, j) \quad (16)$$

And

$$\Phi_y(i, j) = \sin 2o(i, j) \quad (17)$$

Where Φ_x and Φ_y , are the components of the vector field, respectively. With the resulting vector field, the low-pass filtering can then be performed as follows:

$$\Phi'_x(i, j) = \sum_{u=-w_\phi/2}^{w_\phi/2} \sum_{v=-w_\phi/2}^{w_\phi/2} w(u, v) \Phi_x(i - uw, j - vw) \quad (18)$$

And

$$\Phi'_y(i, j) = \sum_{u=-w_\phi/2}^{w_\phi/2} \sum_{v=-w_\phi/2}^{w_\phi/2} W(u, v) \Phi_y(i - uw, j - vw) \quad (19)$$

W is a two-dimensional low-pass filter with unit integral and $w_\phi \times w_\phi$ specifies the size of the filter. Note that the smoothing operation is performed at the block level. For our experiments, we used a mean filter. The smoothed orientation field O' at (i, j) is computed as follows:

$$o'(i, j) = \frac{1}{2} \tan^{-1} \left(\frac{\Phi'_y(i, j)}{\Phi'_x(i, j)} \right) \quad (20)$$

6 Normalization

We normalize the region of interest to a constant mean and variance. Normalization is done to remove the effects of sensor noise and finger pressure differences. Let $I(x, y)$ denote the gray value at pixel (x, y) , M_i and V_i , the estimated mean and variance of each block. $N_i(x, y)$, the normalized gray-level value at pixel (x, y) . For all the pixels in each block, the normalized image is defined as:

$$N_i(x, y) = \begin{cases} M_0 + \sqrt{\frac{(V_0) \times (I(x, y) - M_i)^2}{V_i}}, & I(x, y) > M_i \\ M_0 - \sqrt{\frac{(V_0) \times (I(x, y) - M_i)^2}{V_i}}, & otherwise \end{cases} \quad (21)$$

where M_0 and V_0 are the desired mean and variance values, respectively. Normalization is a pixel-wise operation which does not change the clarity of the ridge and furrow structures. If normalization is done on the entire image, then it cannot compensate for the intensity variations in the different parts of the finger due to finger pressure differences. Normalization of each block separately alleviates this problem.

7 The poincare index value

Many methods have been proposed to detect the singular points in fingerprint images, while the Poincare index which is derived from continuous

curves is the most popular one. As for digital fingerprint images, a double core point has a Poincaré index valued as 1, a core point as 1/2 and a delta point as -1/2 .

Let $\theta(x,y)$ denote the direction of the pixel (x,y) in an $M \times N$ fingerprint image. The Poincaré Index at pixel (x,y) which is enclosed by a digital curve (with N points) can be computed as follows:

$$Poincare(x, y) = \frac{1}{2\pi} \sum_{k=0}^{N-1} \Delta(k) \quad (22)$$

Where

$$\Delta(k) = \begin{cases} \delta(k) & |\delta(k)| < \frac{\pi}{2} \\ \delta(k) + \pi & \delta(k) \leq -\frac{\pi}{2} \\ \pi - \delta(k) & \delta(k) \geq \frac{\pi}{2} \end{cases} \quad (23)$$

$$\delta(k) = \theta(x_{(k+1) \bmod N}, y_{(k+1) \bmod N}) - \theta(x_k, y_k). \quad (24)$$

and it goes in a counter-clockwise direction from 0 to $N-1$. For our method, N is 4 (Fig.6).

$(x-1,y)$	$(x-1,y+1)$
(x,y)	$(x,y+1)$

Fig.6. The mask of detecting singular points

We compute the Poincaré Index at pixel in the (i,j) by the modified version of Poincaré Index(9), and the corresponding value is $Poincare(i,j)$. The modified version of Poincaré Index can present not only the rotation angles, but also the rotation direction of the vector in the vector field, exactly. For our method, the closed digital curve is selected as 4 pixels. In order to calculate simply, the direction yards from 0 to 7 is used to compute the Poincaré Index.

$$\Delta(k) = \begin{cases} \delta(k) & |\delta(k)| < \frac{\pi}{2} \\ \delta(k) + \pi & \delta(k) \leq -\frac{\pi}{2} \\ \delta(k) - \pi & \delta(k) \geq \frac{\pi}{2} \end{cases} \quad (25)$$

8 Singular point detection

If $Poincare(i, j) = 0.5$, the block $M(i,j)$ may contain a core point; If $Poincare(i, j) = -0.5$, the block $M(i,j)$ may contain a delta point; Otherwise, the block $M(i,j)$ doesn't contain singular points.

The blocks which may contain singularities are detected by our method. Then the Poincaré Index at pixel (x,y) which is enclosed by a digital curve of 4 pixels can be compute in the detected blocks(Fig.7), and the corresponding value is $Poincare1(x,y)$. The direction yards from 0 to 7 is also used for computing the Poincaré Index.

If $Poincare1(x, y) = +0.5$, the point is a core point;

If $Poincare1(x, y) = -0.5$, the point is a delta point;

Otherwise, the point is not a singularity.

If the number of core points Nc is more than 2 or the number of delta points Nd is more than 2, we smooth the continuous orientation field until the number of core points or delta points is lesser than 2

The singularity detection algorithm described above has been tested on the fingerprint images in the FVC2002 database. We choose the typical fingerprint image which is shown in Fig.7. In Fig.11, the white blocks contains the core points and the black blocks contains the delta points.



Fig.7. The original fingerprint images



Fig.8 The segmented fingerprint image



Fig.9. The continuous orientation field of fingerprint image

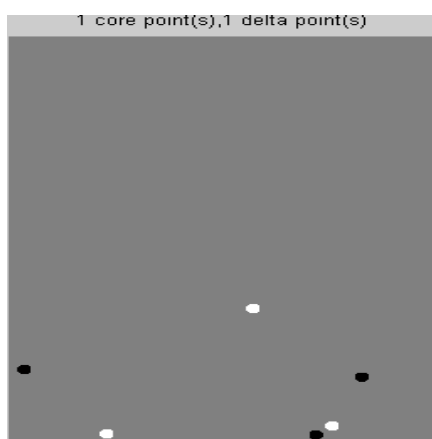


Fig.10. The blocks which may contain singularities:



Fig.11. Singular points found

9 Conclusion

The fingerprints have been traditionally classified into categories based on information in the global patterns of ridges. In large scale fingerprint identification systems, elaborate methods of manual fingerprint classification systems were developed to index individuals into bins based on classification of their fingerprints; these methods of binning eliminate the need to match an input fingerprint to the entire fingerprint database in identification

applications and significantly reduce the computing requirements. Efforts in automatic fingerprint classification have been exclusively directed at replicating the manual fingerprint classification system. A fingerprint classification system should be invariant to rotation, translation, and elastic distortion of the frictional skin. Although fingerprint landmarks provide very effective fingerprint class clues, methods relying on the fingerprint landmarks alone may not be very successful due to lack of availability of such information in many fingerprint images and due to the difficulty in extracting the landmark information from the noisy fingerprint images. As a result, the most successful approaches need to (I) supplement the orientation field information with ridge information; (II) use fingerprint landmark information when available but devise alternative schemes when such information cannot be extracted from the input fingerprint images; and (III) use reliable structural/syntactic pattern recognition methods in addition to statistical methods.

Fingerprint identification in a large dataset is a very time consuming task. Fingerprint indexing can evidently reduce the number of comparisons. SPs can be robustly identified and contain fingerprint intrinsic features.

Several approaches have been developed for automatic fingerprint classification. These approaches can be broadly categorized into four main categories:

- 1)_ model-based,
- 2)_ structure-based,
- 3)_ frequency-based, and
- 4)_ syntactic.

The model-based fingerprint classification technique uses the locations of singular points (core and delta) to classify a fingerprint into the five above-mentioned classes. A model-based approach tries to capture the knowledge of a human expert by deriving rules for each category by hand constructing the models and therefore, does not require training.

In this paper, a novel method based on the point orientation field and the block orientation field is presented with a higher accuracy to overcome the shortcoming of the traditional methods. The main benefit of this algorithm is its fast running speed, because we don't have to calculate the Poincaré Index value at every pixel and only detect the singularities in the effective region. Experimental results for real fingerprint images shows that the proposed method provides accurate results, which would facilitate fingerprint identification and fingerprint classification afterwards.

References:

- [1] H. C. Lee and R. E. Gaensslen, *Advances in Fingerprint Technology*. Elsevier, New York (1991).
- [2] B. Miller, Vital signs of identity, *IEEE Spectrum* 31(2), 22-30 (1994).
- [3] N. Ratha, S. Chen and A. K. Jain, Adaptive flow orientation based texture extraction in fingerprint images, *Pattern Recognition*, 28, 1657-1672 (1995)
- [4] PANKANTI S, PRABHAKAR S, JAIN A K. On the individuality of fingerprints[J].*IEEE Transactions on PAMI*, 2002, 24(8) : 1010-1025.
- [5] Lin Hong. Automatic Personal Identification Using Fingerprints, Ph.D. Thesis,1998.
- [6] Tan TZ, Ning XB, Yin YL, Zhan XS, Chen Y. A method for singularity detection in fingerprint images[J]. *Journal of Software*, 2003, 14(6):1082-1088.
- [7] R. Cappelli, A. Lumini, D. Maio, D. Maltoni, Fingerprint classification by directional image partitioning, *Trans. Pattern Anal. Mach. Intell.* 21 (5) (1999) 402 - 421.
- [8] M.J. Donahue, S.I. Rokhlin, On the use of level curves in image analysis, *Image Understanding* 57 (3) (1993) 185 - 203.
- [9] S. Ando, Consistent gradient operators, *IEEE Trans. Pattern Anal. Machine Intelligence* 20 (3) (2000) 252-265
- [10] M. Kass, A. Witkin, Analyzing oriented patterns, *Computer Vision Graphics Image Processing* 37 (1987) 362-385.
- [11] B. Jahne, *Digital Image Processing-Concepts, Algorithms and Scientific Applications*, 4th Edition, Springer, Berlin Heidelberg, 1997.
- [12] L. Ji, H. Yan, Attractable snakes based on the greedy algorithm for contour extraction, *Pattern Recognition* 35 (2) (2002) 791-806.
- [13] He YL, Tian J. Image enhancement and minutia matching algorithms in automated fingerprint verification[J]. *Pattern Recognition Letters*, 2003, 24(9-10): 1349-1360.
- [14] Nie G J, Wu C. Studies on continuously distributed directional image in automated fingerprint identification [J]. *Journal of Image and Graphics*,2005,10(3):315-319.
- [15] M. Kass and A. Witkin, "Analyzing oriented patterns," *Comput. Vis. Graph. Image Processing*, vol. 37, no. 4, pp. 362-385, 1987.
- [16] T. Chang, "Texture analysis of digitized fingerprints for singularity detection," in *Proc. 5th Int. Conf. Pattern Recognition*, 1980, pp. 478-480.
- [17] M. Kawagoe and A. Tojo, "Fingerprint pattern classification," *Pattern Recognize.*, vol. 17, no. 3, pp. 295-303, 1984.
- [18] A. R. Rao, *A Taxonomy for Texture Description and Identification*, New York: Springer-Verlag, 1990.
- [19] L. Hong, Y. Wan, and A. K. Jain, "Fingerprint image enhancement: Algorithm and performance evaluation," *IEEE Trans. Pattern Anal. Machine Intell.*, vol. 20, pp. 777-789, Aug. 1998
- [20] K. Woods, W.P. Kegelmeyer, and K.W. Bowyer, "Combination of Multiple Classifiers Using Local Accuracy Estimates," *IEEE Trans. Pattern Analysis and Machine Intelligence*, vol. 19, no. 4, pp. 405-410, Apr. 1997.
- [21] CAPPELLI, R, LUMINI, A, MAIO, D., and MALTONI, D.(1999): Fingerprint Classification by Directional Image Partitioning[J]. *IEEE Trans. On Pattern Analysis and Machine Intelligence* 21(5):402-421.
- [22] R. O. Duda, P. E. Hart, and D.G. Stork, *Pattern Classification*, 2nd Edition, John Wiley & Sons, November 2000.
- [23] D. Maltoni, D. Maio, A. K. Jain, S. Prabhaker. *Handbook of Fingerprint Recognition*. Springer, New York, 2003.
- [24] Zhang W W, Wang S, Wang Y S. Structure matching algorithm of fingerprint minutia based on core point[J]. *Acta Automatica Sinica*, 2003, 29(6):842-850.
- [25] Wang L, Dai M. Localization of singular points in fingerprint images based on the Gaussian-Hermite moments[J]. *Journal of Software*, 2006, 17(2):242-249.
- [26] G. Giacinto, F. Roli, Ensembles of neural networks for soft classification of remote sensing images, in: *Proceedings of the European Symposium on Intelligent Techniques*, 1997, pp. 166 - 170.
- [27] G. Giacinto, F. Roli, L. Bruzzone, Combination of neural and statistical algorithms for supervised classification of remote-sensing images, *Pattern Recognition Lett.* 21 (5) (2000).
- [28] J. Kittler, F. Roli (Eds.), *Proceedings of the First International Workshop on Multiple Classifier Systems*, Lecture Notes in Computer Science, Vol. 1857, Springer, New York, 2000.
- [29] J. L. Blue, G. T. Candela, P. J. Grother, R. Chellapa and C. L. Wilson, Evaluation of pattern classifiers for fingerprint and OCR applications, *Pattern Recognition* 27(4), 485-501 (1994).
- [30] C. L. Wilson, G. T. Candela and C. I. Watson, *Neural Network Fingerprint Classification*, J.

- Artific. Neural Networks 1(2), 1-25 (1993).
- [31] R. M. Stock and C. W. Swonger, Development and evaluation of a reader of fingerprint minutiae, Cornell Aeronautical Laboratory, Technical Report CAL No. XM-2478-X-1 : 13-17 (1969).
 - [32] C. I. Watson and C. L. Wilson, NIST Special Database 4. Fingerprint Database. National Institute of Standard and Technology (March 1992).
 - [33] C. I. Watson, NIST Special Database 9. Mated Fingerprint Card Pairs. National Institute of Standard and Technology (February 1993).
 - [34] C.I. Watson, P.J. Grother, and D.P. Casasent, "Distortiontolerant filter for elastic-distorted fingerprint matching", Proc. SPIE Vol. 4043, pp. 166-174, 2000.
 - [35] B.V.K. Vijaya Kumar, M. Savvides, K. Venkataramani, and C.Y. Xie, "Spatial frequency domain image processing for biometric recognition", Image Processing, Proc. Int. Conf. on, Volume 1, pp. I-53 - I-56, Sept. 2002.
 - [36] C. Park, S. Oh, D. Kwak, B. Kim, Y Song, and K Park, "A new reference point detection algorithm based on orientation pattern labeling in fingerprint images", pp. 697-703, Pattern Recognition and Image Analysis, First Iberian Conference, IbPRIA 2003.